Environ. Sci. Technol. **1999**, *33,* 1931−1935

Calcium Bisulfite Oxidation Rate in the Wet Limestone−Gypsum Flue Gas Desulfurization Process

AMEDEO LANCIA*,† AND DINO MUSMARRA‡

Dipartimento di Ingegneria Chimica, Università di Napoli "Federico II", p.le Tecchio 80, 80125 Napoli, Italy, and Istituto di Ricerche sulla Combustione, CNR, p.le Tecchio 80, 80125 Napoli, Italy

In this paper oxidation of calcium bisulfite in aqueous solutions was studied, in connection with the limestone−gypsum flue gas desulfurization process. Experimental measurements of the oxidation rate were carried out in a laboratory scale stirred reactor with continuous feeding of both gas and liquid phase. A calcium bisulfite clear solution was used as liquid phase, and pure oxygen or mixtures of oxygen and nitrogen were used as gas phase. Experiments were carried out at $T = 45$ °C varying the composition of the liquid phase and the oxygen partial pressure. Manganous sulfate was used as catalyst. The analysis of the experimental results showed that the kinetics of bisulfite oxidation in the presence of $MnSO_4$ follow a parallel reaction mechanism, in which the overall reaction rate can be calculated as the sum between the uncatalyzed rate ($^3/_2$ order in bisulfite ion) and the catalyzed reaction rate (first order in manganous ion).

Introduction

The wet limestone−gypsum process is the most common flue gas desulfurization treatment. The byproduct of this process is a solid mixture mostly made of $CaSO_3 \cdot {}^1/_2H_2O$. However, if sulfite and bisulfite ions are oxidized prior solid formation, a precipitate mostly made of $CaSO_4 \cdot 2H_2O$ (gypsum) is obtained. Production of gypsum is useful not only because it is inert (while $CaSO_3 \cdot {}^1/_2H_2O$ has a considerable chemical oxygen demand) but also because it can be sold as a building material it the market specifications are met. The overall reactions for oxidation of sulfite and bisulfite ions in aqueous solutions are

$$SO_3^{2-} + {}^1/_2O_2 = SO_4^{2-} \quad (1)$$

$$HSO_3^{-} + {}^1/_2O_2 = SO_4^{2-} + H^+ \quad (2)$$

The kinetics of such reactions, and particularly of the absorption of oxygen by basic solutions of sodium sulfite in the presence of catalysts, received great attention during the past decades; Linek and Vacek (*1*) presented a detailed review of the literature for the period 1960−1980. The researchers who studied the reaction of sulfite oxidation pointed out the extreme sensitivity of its kinetics to experimental conditions, which often prevented the achievement of reproducible results. It has been shown that liquid-phase composition (sulfite concentration, dissolved oxygen, pH), temperature, and the presence, even in traces, of catalysts (Co^{2+}, Cu^{2+}, Mn^{2+}) and inhibitors (alcohols, phenols, hydroquinone) strongly affect the reaction rate.

Sulfite oxidation was studied both in homogeneous conditions, obtained by contacting a sulfite solution with an oxygen saturated solution, and in heterogeneous conditions, obtained by contacting a sulfurous solution with an oxygen containing gas phase. Results for homogeneous conditions are relatively consistent. Working with high sulfite concentrations Yagi and Inoue (*2*) and Srivastva et al. (*3*) found a first-order kinetic equation with respect to both oxygen and sulfite. On the other hand, results obtained with lower concentrations, indicate a $^3/_2$-order dependence from sulfite and a zero-order dependence from oxygen, both in the absence and in the presence of such catalysts as copper, manganese, and cobalt (*4*−*9*). The dependence of the reaction rate on the catalyst concentration is more uncertain; while the reaction rate is proportional to the square root of the concentration of Co^{2+} or Mn^{2+}, the description of the catalytic activity of copper appears more difficult (*10*).

On the basis of the results reported in the literature (*4*−*9*, *11*−*12*), for a pH range of 7.5−9, low sulfite concentration and Co^{2+} or Mn^{2+} as catalyst, the following equation appears the most appropriate to describe the kinetics of the oxidation reaction

$$r = k c_M^{1/2} c_{S(IV)}^{3/2} \quad (3)$$

where r is the reaction rate expressed as moles of SO_4^{2-} produced per unit time and volume, k is the kinetic constant, c_M the catalyst concentration, and $c_{S(IV)}$ the total sulfite concentration. However, the values found for the kinetic constant k are not at all consistent: in particular the reported values of k at 25 °C range between 2 and 35×10^6 m^3/mol s, while the activation energy ranges from 50 to 150 kJ/mol.

Equation 3 can be interpreted by making the hypothesis that the reaction takes place via a free radical mechanism, with a chain initiated by the catalyst autoxidation from M^{z+} to $M^{(z+1)+}$ or by the action of UV light (*13*). Such hypothesis is also strengthened by the extreme sensitivity of the reaction rate to such free radicals scavengers as alcohols, phenols, and hydroquinone (*14*−*17*). The mechanism best documented for the reaction is the one proposed by Bäckstrom (*11*, *18*, *19*), which considers the free radicals SO_3^- and SO_5^- as chain carriers.

More recently the study of sulfite oxidation in heterogeneous conditions received great attention, since these conditions are closer to those encountered in FGD processes, where the reaction is carried out by bubbling air into a solution saturated with respect to calcium sulfite at pH 3.5−5 (*20*). In FGD plants, due to the lower pH, the prevailing sulfurous species is bisulfite ion HSO_3^- instead of sulfite ion SO_3^{2-}; besides, since calcium sulfite solubility is rather low, the concentrations involved in the reaction are lower than those taken into account by the researchers whose work is described above. However, the interpretation of the results relative to heterogeneous conditions is more complex, due to the interactions between chemical reactions and diffusive transport of reactants, products, and catalysts (*21*). Barron and co-workers (*6*, *22*) proposed an interpretation according to which, when the absorption rate is high, the overall reaction is controlled by the rate of production of the activated form of the catalyst, $M^{(z+1)+}$. More recently Lancia et al. (*12*) studied the heterogeneous oxidation of calcium bisulfite in conditions

* Corresponding author phone: [39] (81)768-2243; fax: [39] (81)-593-6939; e-mail: lancia@unina.it.
† Università di Napoli "Federico II".
‡ Istituto di Ricerche sulla Combustione.

10.1021/es9805425 CCC: $18.00
Published on Web 04/24/1999

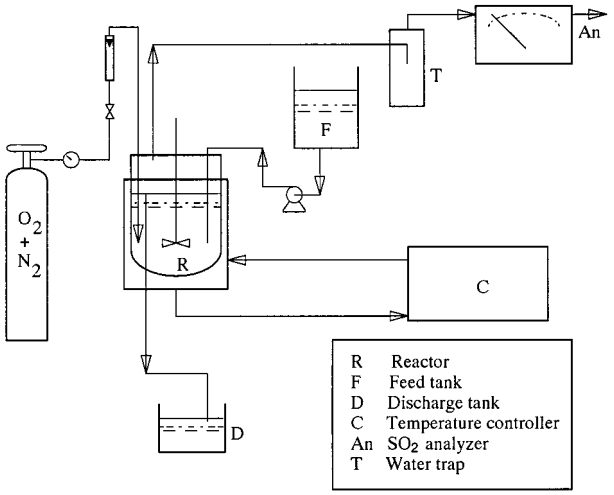

FIGURE 1. Sketch of the experimental apparatus.

of pH and temperature comparable to those encountered in the wet limestone FGD process. They showed that in the absence of catalyst the oxidation rate is $^3/_2$-order in bisulfite ion and zero-order in oxygen.

With the aim of gathering a better understanding of the fundamental phenomena involved in forced oxidation, in the present paper the attention is focused on catalytic oxidation of calcium bisulfite. An experimental work is presented in which heterogeneous conditions are considered, and pure oxygen or mixtures of oxygen and nitrogen are used as gas phase. Experiments were performed in the slow reaction regime (*23*) using manganous sulfate as catalyst. The experimental findings are compared with those previously obtained operating in absence of catalyst (*12*), with the aim of obtaining a kinetic equation for the catalyzed rate of reaction.

Experimental Apparatus and Procedure

The rate of calcium bisulfite oxidation was measured using the laboratory scale apparatus sketched in Figure 1. Such an apparatus consists of a thermostated stirred reactor with lines for continuous feeding and discharging of both gas and liquid phase. The reactor, made of Pyrex glass, is a jacketed, 0.13 m i.d. cylinder with a hemispherical bottom, fitted with two vertical baffles and a liquid overflow. A four flat blade axial stirrer (0.01 m blade width, 0.05 impeller diameter) was used to provide thorough mixing in the liquid phase. The stirrer speed was kept constant in the experiments at 13.3 s^{-1}.

The temperature was set in all experiments at 45 °C. The gas phase was pure oxygen or mixtures of oxygen and nitrogen with oxygen concentrations in the range of 5−40%; it was taken from cylinders and bubbled at the bottom of the reactor. The volumetric flow rate of the gas fed to the reactor, measured by a rotameter, was kept constant at 1.39×10^{-4} m^3/s. Such gas flow rate, in conjunction with the stirrer speed of 13.3 s^{-1}, gave a liquid holdup of 3.9×10^{-4} m^3. The calculated impeller power input, taking into account the presence of gas bubbles, is about 0.55 W (*24*, *25*).

The liquid phase was a clear solution prepared by dissolving analytical grade calcium hydroxide into analytical grade sulfur dioxide in solution and by diluting with bidistilled water. The Ca^{2+} concentration ranged from 1 to 40 mol/m^3, while the total S(IV) concentration ranged from 0.1 to 55 mol/m^3, with a pH in the range of 2.0−4.0. Manganous sulfate ($MnSO_4$) in solution was used as a homogeneous catalyst, and its concentration was varied in the range of 0.01−1.4 mol/m^3. The liquid flow rate was kept constant at the value of 8.5×10^{-7} m^3/s in each experiment, corresponding to a mean residence time into the reactor t of about 460 s.

At the beginning of each experiment, as soon as the liquid in the reactor reached the overflow, agitation was started and the gas stream was introduced. It was assumed that steady state was reached after a time longer than 5t had elapsed. The oxidation rate at steady state was evaluated by measuring the total sulfate concentration both in the inlet and in the outlet liquid streams. Furthermore, in both streams the concentrations of total sulfite and Ca^{2+} ion were measured. Total sulfite concentration was measured by iodometric titration using starch as an indicator, Ca^{2+} ion concentration was measured by EDTA titration using muresside as an indicator, while the total sulfate concentration was measured by means of a turbidimeter (Hach DR/3) at 450 nm wavelength.

Experimental Results

Three different series of experiments were carried out to measure the reaction rate of calcium bisulfite oxidation in the presence of manganous sulfate as catalyst. In the first series the total sulfite concentration was varied within quite a broad range while keeping oxygen partial pressure (p_{O^2}) fixed at 0.21 atm and using two different concentrations of Mn^{2+} ion. In the second series the manganous concentration $c_{Mn^{2+}}$ was varied in the range of 0.009−2 mol/m^3 while keeping p_{O^2} fixed at 0.21 atm and the total sulfite concentration below 7 mol/m^3. Eventually, in the third series, different oxygen concentrations in the gas phase were considered for two values of Mn^{2+} concentration, with the total sulfite concentration below 7 mol/m^3. The experimental results for the three series of experiments are reported in Tables 1−3 where, together with the reaction rate, there are reported the total concentrations of sulfite, sulfate calcium, and manganese.

To find a kinetic equation from the experimental results, it has been necessary to speciate the solution composition. With this aim the equilibrium equations for the following reactions were used (see Appendix)

$$SO_{2(aq)} + H_2O = H^+ + HSO_3^- \quad (4)$$

$$HSO_3^- = H^+ + SO_3^{2-} \quad (5)$$

$$HSO_4^- = H^+ + SO_4^{2-} \quad (6)$$

$$H_2O = H^+ + OH^- \quad (7)$$

for which the values of the thermodynamic equilibrium constants were calculated using data reported by Goldberg and Parker (*26*, reactions 4 and 5) and by Brewer (*27*, reactions 6 and 7). Together with the equilibrium equations relative to reactions (*4*−*7*), the stoichiometric equations for total sulfite and total sulfate concentrations and the electroneutrality equation were considered

$$c_{SO_{2(aq)}} + c_{HSO_3^-} + c_{SO_3^{2-}} = c_{S(IV)} \quad (8)$$

$$c_{HSO_4^-} + c_{SO_4^{2-}} = c_{S(VI)} \quad (9)$$

$$\sum_I z_I c_I = 0 \quad (10)$$

where z_I is the electric charge of the I species, with I = Ca^{2+}, H^+, HSO_3^-, SO_3^{2-}, HSO_4^-, SO_4^{2-}, OH^-, and Mn^{2+}.

In Figure 2 the results of the first experimental series are reported as reaction rate versus the bisulfite ion concentration, the value of which was evaluated by means of eqs 4−10. To make a comparison with the results obtained in absence of catalyst, in Figure 2 there are also included the results previously reported by Lancia et al. (*12*). The "uncatalyzed"

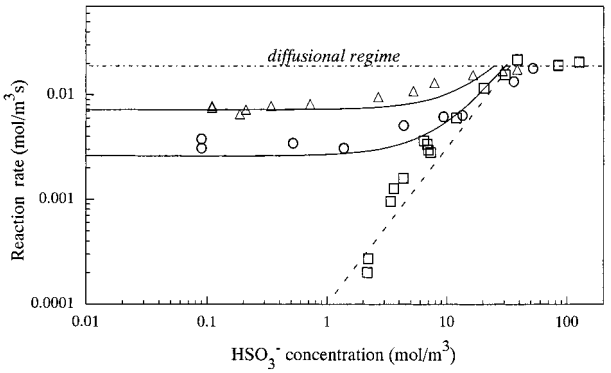

FIGURE 2. Reaction rate versus HSO_3^- concentration for experiments carried out with oxygen partial pressures of 0.21 atm. (□) $c_{Mn^{2+}}$ = 0 (ref *12*); (○) $c_{Mn^{2+}}$ = 0.018 mol/m³; (△) $c_{Mn^{2+}}$ = 0.050 mol/m³. (- -) eq 12; (- · -) eq 11; (—) eq 15.

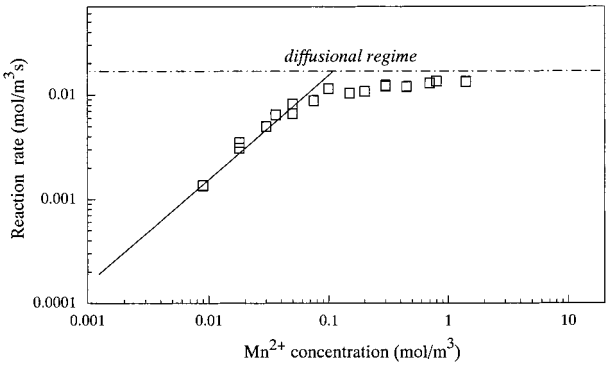

FIGURE 3. Reaction rate versus Mn^{2+} concentration for experiments carried out with p_{O_2} = 0.21 atm and with $c_{HSO_3^-} < 7.0$ mol/m³. (- · -) eq 11; (—) eq 15.

results show that the reaction rate has a $^3/_2$-order dependence on bisulfite ions, and it grows with $c_{HSO^{3-}}$ until it reaches an upper limit where it no longer depends on $c_{HSO_3^-}$. Figure 2 also shows that Mn^{2+} has a marked catalytic effect, which is particularly evident at relatively low HSO_3^- concentrations ($c_{HSO_3^-} < 7$ mol/m³), while it tends to become less evident at higher values of $c_{HSO_3^-}$, where the difference between the "catalyzed" and the "uncatalyzed" reaction rate is almost negligible. The reaction rates relative to the second experimental series are reported in Figure 3 as a function of $c_{Mn^{2+}}$. This figure shows that the reaction rate increases when $c_{Mn^{2+}}$ increases, until an upper limit is reached, in which r becomes almost independent of $c_{Mn^{2+}}$. Eventually, results relative to the third experimental series, obtained by varying the oxygen partial pressure in the gas phase, are reported in Figure 4a, showing that the influence of oxygen partial pressure on r is practically negligible. Similar results obtained in uncatalyzed conditions (*12*) are shown in Figure 4b.

Discussion

Since sulfite oxidation interacts with gas—liquid diffusive transport of oxygen, the analysis of the experimental results is made complex by the problem of individuating the regime in which oxygen absorption takes place. The fact that for low HSO_3^- or Mn^{2+} concentrations the reaction rate depends on liquid-phase composition, while for higher concentrations it becomes independent of the composition, indicates that, when such concentrations are increased beyond a certain value, the transition from the *kinetic subregime* to the *diffusional subregime* takes place (*23*). In the kinetic subregime the oxygen absorption rate and the reaction rate coincide, and therefore the experimental results can be directly used to individuate the kinetic equation for the

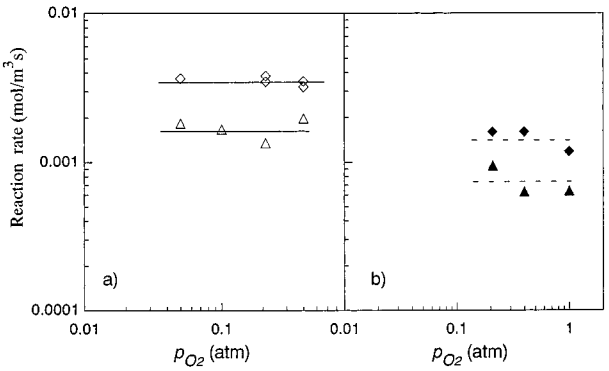

FIGURE 4. Reaction rate versus O_2 partial pressure. (a) $c_{HSO_3^-} < 7.0$ mol/m³; (△) $c_{Mn^{2+}}$ = 0.010 mol/m³; (◇) $c_{Mn^{2+}}$ = 0.018 mol/m³; (—) eq 15. (b) $c_{Mn^{2+}}$ = 0; (▲) $c_{HSO_3^-}$ = 2.8 mol/m³; (◆) $c_{HSO_3^-}$ = 5.5 mol/m³; (- -) eq 12 (ref *12*).

oxidation reaction; on the other hand, when the process takes place in the diffusional subregime, its overall rate becomes independent of liquid-phase composition and is only controlled by the kinetics of diffusive oxygen absorption (*28*). Therefore the data relative to the right sides of Figures 2 and 3, which appear to be relative to experiments in which the transition from the kinetic to the diffusional subregime took place, can be described by means of the following equation, which Astarita (*23*) indicates as characteristic of the diffusional subregime:

$$r = 2k^{o}_{L}ac^{i}_{O_2} \qquad (11)$$

In this equation $c^{i}_{O_2}$ is the interfacial oxygen concentration, which can be evaluated by means of the Henry law and $k^{o}_{L}a$ is the product between the liquid side mass transfer coefficient and the specific gas—liquid contact area. This latter, equal to 411 m^{-1}, has been experimentally evaluated in a previous paper (*29*) where the same fluidodynamic conditions were adopted. Using the data relative to the right side of Figures 2 and 3 and the value of 1.02×10^5 m³Pa/mol for the Henry constant for O_2 at 45 °C (*30*), it is possible to estimate the value of $k^{o}_{L}a$ for the experimental conditions considered in the present work. In particular the value of 3.02×10^{-2} s^{-1} was found; this value is close to that evaluated by a dimensionless correlation proposed by Anselmi et al. (*31*) using a reactor similar to the one used in the present work. Using the value of $k^{o}_{L}a$ experimentally obtained, the horizontal straight lines reported in Figures 2 and 3 were obtained.

The results relative to the left sides of Figures 2 and 3, i.e. those obtained in conditions of kinetic subregime (Hatta number varying in the range $4.8 \times 10^{-2} \div 1.5 \times 10^{-1}$), can be used to evaluate the kinetic equation of the oxidation reaction in the experimental conditions considered. In particular, for what concerns the "uncatalyzed" oxidation rate r_u, the following equation was found by Lancia et al. (*12*), zero-order in the concentration of dissolved oxygen and $^3/_2$-order in the concentration of the bisulfite ion

$$r_u = k_u c^{3/2}_{HSO_3^-} \qquad (12)$$

where k_u is the kinetic constant relative to uncatalyzed oxidation, the value of which is 0.96×10^{-4} m$^{3/2}$/mol$^{1/2}$ s at 45 °C.

For what concerns the catalytic effect of Mn^{2+}, the results reported in Figure 2 show that for low values of $c_{HSO_3^-}$ the reaction rate, while lower than the "diffusional" rate, is definitely higher than the uncatalyzed rate; for higher values of $c_{HSO^{3-}}$ the reaction rate becomes practically coincident with the uncatalyzed rate given by eq 12, and eventually for high values $c_{HSO^{3-}}$ it reaches the "ceiling" fixed by the transition

TABLE 1. Experimental Results for Oxygen Partial Pressure of 0.21 atm and $c_{Mn^{2+}} = 0.018$ and 0.05 mol/m³

no.	$c_{Mn^{2+}}$ (mol/m³)	p_{O_2} (atm)	$c_{S(IV)}$ (mol/m³)	$c_{S(VI)}$ (mol/m³)	$c_{Ca^{2+}}$ (mol/m³)	$r \times 10^3$ (mol/m³ s)
1	0.018	0.21	0.1	3.09	1.35	3.1
2	0.018	0.21	0.1	3.32	1.35	3.1
3	0.018	0.21	0.1	3.32	1.35	3.8
4	0.018	0.21	0.63	2.7	1.35	3.46
5	0.018	0.21	0.63	2.7	1.35	3.5
6	0.018	0.21	1.62	3.29	2.71	3.1
7	0.018	0.21	5.17	4.67	5.4	5.13
8	0.018	0.21	10.8	4.71	8.11	6.2
9	0.018	0.21	15.3	5.26	10.8	6.39
10	0.018	0.21	36.3	9.33	27	13.4
11	0.018	0.21	55.5	15.5	40.5	17.9
12	0.05	0.21	0.13	3.94	2.7	7.59
13	0.05	0.21	0.13	4.21	2.7	7.9
14	0.05	0.21	0.21	4.06	2.7	6.62
15	0.05	0.21	0.26	4.94	3.24	7.27
16	0.05	0.21	0.51	7.9	3.78	7.87
17	0.05	0.21	1.01	7.56	4.32	8.2
18	0.05	0.21	3.64	7.31	5.4	9.61
19	0.05	0.21	6.52	7.81	8.11	10.9
20	0.05	0.21	11	11.06	10.8	13.1
21	0.05	0.21	20.1	10.36	16.2	15.5
22	0.05	0.21	39.4	10.84	21.6	17
23	0.05	0.21	50.3	11.28	27	17.6

TABLE 2. Experimental Results for Oxygen Partial Pressure of 0.21 atm and Different Mn^{2+} Concentrations

no.	$c_{Mn^{2+}}$ (mol/m³)	p_{O_2} (atm)	$c_{S(IV)}$ (mol/m³)	$c_{S(VI)}$ (mol/m³)	$c_{Ca^{2+}}$ (mol/m³)	$r \times 10^3$ (mol/m³ s)
24	0.03	0.21	5.05	4.05	3.81	4.98
25	0.036	0.21	4.93	4.32	4.32	6.42
26	0.036	0.21	5.45	4.92	4.15	6.5
27	0.05	0.21	0.21	4.06	2.7	6.62
28	0.05	0.21	1.01	7.56	2.7	8.2
29	0.075	0.21	5.05	6.09	4.32	8.82
30	0.1	0.21	3.03	7.54	4.32	11.5
31	0.15	0.21	9.85	7.12	8.1	10.4
32	0.2	0.21	4.55	7.31	4.32	10.8
33	0.3	0.21	2.25	9.2	4.32	12.1
34	0.3	0.21	9.6	9.73	10.8	12.4
35	0.45	0.21	13.39	9.97	9.73	12
36	0.7	0.21	1.27	11.2	5.4	13
37	0.8	0.21	16.7	11.4	10.8	13.5
38	1.4	0.21	14.65	20.8	11.9	13.4

TABLE 3. Experimental Results for $c_{Mn^{2+}} = 0.01$ and 0.018 mol/m³ and Different Oxygen Partial Pressures

no.	$c_{Mn^{2+}}$ (mol/m³)	p_{O_2} (atm)	$c_{S(IV)}$ (mol/m³)	$c_{S(VI)}$ (mol/m³)	$c_{Ca^{2+}}$ (mol/m³)	$r \times 10^3$ (mol/m³ s)
39	0.01	0.05	1.77	1.31	1.35	1.83
40	0.01	0.1	3.79	1.47	2.16	1.67
41	0.01	0.21	2	1.5	1.35	1.35
42	0.01	0.4	3.16	2.2	2.7	1.98
43	0.018	0.05	0.1	3.37	1.35	3.67
44	0.018	0.05	2.12	3.16	2.7	3.67
45	0.018	0.21	0.63	2.7	1.35	3.49
46	0.018	0.21	0.1	3.32	1.35	3.8
47	0.018	0.4	2.8	2.58	2.07	3.51

to the diffusional subregime. Such a dependence of r on $c_{HSO_3^-}$ indicates that a parallel reaction mechanism exists, with the following kinetic equation

$$r = r_u + r_c \tag{13}$$

where r_u is given by eq 12, and r_c is the "catalyzed" reaction rate.

TABLE 4. Debye–Hückel Parameters for Eqs (A4–5) (Ref 33)

species	B
H^+	0.087
OH^-	−0.012
HSO_3^-	−0.013
SO_3^{2-}	−0.087
HSO_4^-	−0.013
SO_4^{2-}	−0.09
Ca^{2+}	−0.035

The left part of Figure 2, which is characterized by the fact that the "uncatalyzed" contribution is negligible in comparison with the overall rate, shows that r_c seems independent of the bisulfite ion concentration. The results reported in Figure 3, which refer to experiments carried out with $p_{O_2} = 0.21$ atm and with HSO_3^- concentration low enough to have a negligible uncatalyzed rate, show a linear dependence of r_c on $c_{Mn^{2+}}$. Furthermore, the results of the experiments reported in Figure 4 show that the reaction rate does not depend on the oxygen partial pressure, and, therefore, on the concentration of dissolved oxygen; however, for higher oxidation rates p_{O_2} does play a role, albeit indirectly, by determining the transition from the kinetic to the diffusional subregime.

The concentrations evaluated by means of eqs 4–10 were used in a regression analysis to find a power law kinetic equation for bisulfite oxidation in the presence of manganous as catalyst. By means of this analysis, performed over all ionic species, it was concluded that the only species significantly affecting the oxidation rate is the manganous ion. The regression analysis, with a correlation coefficient (R^2) equal to 0.88, leads to a kinetic equation of order zero with respect to both dissolved oxygen and bisulfite ion and of order one with respect to manganous ion, so that it is possible to write

$$r_c = k_c c_{Mn^{2+}} \tag{14}$$

with $k_c = 0.145\ s^{-1}$. Considering eq 12 together with eq 14, the overall kinetic equation for bisulfite oxidation is

$$r = k_u c_{HSO^{3-}}^{3/2} + k_c c_{Mn^{2+}} \tag{15}$$

Equation 15 is reported as a continuous line in Figures 2–4, and it appears that there is a very good agreement between such an equation and the experimental data. However it has to be pointed out that the problem of individuating a consistent kinetic mechanism capable of interpreting eq 15 remains open.

Glossary

A_γ	Debye–Hückel constant, $m^{3/2}/mol^{1/2}$
a	specific interfacial area, m^{-1}
a_I	activity of the I species, mol/m^3
B	Debye–Hückel parameter
c_I	concentration of the I species, mol/m^3
c^i_I	interfacial concentration of the I species, mol/m^3
F	ionic strength, mol/m^3
Ha	Hatta number, dimensionless
K	equilibrium constant
k	kinetic constant, $m^3/mol\ s$
k_L^o	liquid side mass transfer coefficient, m/s
p_I	partial pressure of the I species, Pa
r	reaction rate, $mol/m^3 s$

R correlation coefficient, dimensionless

T temperature, °C

z_I electric charge of the I species, dimensionless

Greek Symbols

a_I stoichiometric coefficient of the I species, dimensionless

γ_I activity coefficient of the I species, dimensionless

τ liquid-phase mean residence time, s

Subscripts

c catalyzed

M cation

u uncatalyzed

c anions

Appendix

The chemical reactions taken into account can be written in the following general form

$$\sum_I \alpha_I I = 0 \quad \text{(A1)}$$

where a_I is the stoichiometric coefficient of the I species and is assumed positive for the reactants and negative for the products. The equilibrium condition for reaction A1 is

$$K = \prod_I a_I^{-\alpha} I \quad \text{(A2)}$$

where a_I is the activity of the I species.

The activity a_I is related to the molar concentration by

$$a_I = c_I \gamma_I \quad \text{(A3)}$$

where g_I is the activity coefficient.

Values of the activity coefficients for cations (M) and anions (x) can be calculated by means of the extended version of the Debye−Hückel theory proposed by Bromley and coworkers (*32*). According to those authors it is

$$\log(\gamma_M) = -\frac{A_\gamma z_M (F)^{1/2}}{1 + (F)^{1/2}} + B_M \sum_x c_x + \sum_x B_x c_x \quad \text{(A4)}$$

$$\log(\gamma_x) = -\frac{A_\gamma z_M (F)^{1/2}}{1 + (F)^{1/2}} + B_x \sum_M c_M + \sum_M B_M c_M \quad \text{(A5)}$$

where A_g is the Debye−Hückel constant, the value of which is 5.62×10^{-2} m$^{3/2}$ mol$^{-1/2}$ (*33*), and F is the ionic strength, which can be evaluated by means of the following equation:

$$F = \frac{1}{2} \sum_I z_I^2 c_I \quad \text{(A6)}$$

The values of the Debye−Hückel parameters B are reported in Table 4, taken from Abdulsattar et al. (*33*).

Literature Cited

(1) Linek, V.; Vacek, V. *Chem. Eng. Sci.* **1981**, *36*, 1747−1768.
(2) Yagi, S.; Inoue, H. *Chem. Eng. Sci.* **1962**, *17*, 411−421.
(3) Srivastava, R. D.; McMillan, A. F.; Harris, I. J. *Can. J. Chem. Eng.* **1968**, *46*, 181−184.
(4) Barron, C. H.; O'Hern, H. A. *Chem. Eng. Sci.* **1966**, *21*, 397−404.
(5) Matsuura, A.; Harada, J.; Hakehata, T.; Shirai, T. *J. Chem. Eng. Jpn.* **1969**, *2*, 199−203.
(6) Chen, T. I.; Barron, C. H. *Ind. Eng. Chem. Fundam.* **1972**, *11*, 466−470.
(7) Mishra, G. C.; Srivastava, R. D. *Chem. Eng. Sci.* **1975**, *30*, 1387−1390.
(8) Mishra, G. C.; Srivastava, R. D. *Chem. Eng. Sci.* **1976**, *31*, 969−971.
(9) Bengtsson, S.; Bjerle, I. *Chem. Eng. Sci.* **1975**, *30*, 1429−1435.
(10) Greenhalgh, S. H.; McManamey, W. J.; Porter, K. E. *Chem. Eng. Sci.* **1975**, *30*, 155−157.
(11) Hayon, E.; Trenin, A.; Wilf, J. *J. Am. Chem. Soc.* **1972**, *94*, 47−57.
(12) Lancia, A.; Musmarra, D.; Pepe, F. *Chem. Eng. Sci.* **1996**, *16*, 3889−3896.
(13) Bäckstrom, H. L. J. *J. Am. Chem. Soc.* **1927** *49*, 1460−1472.
(14) Alyea, N.; Bäckstrom, H. L. J. *J. Am. Chem. Soc.* **1929**, *51*, 90−109.
(15) Altwicker, E. R. *Trans. I Chem E* **1977**, *55*, 281−282.
(16) Braga, T. G.; Connick, R. E. In *Flue Gas Desulfurization*; Hudson, J. L., Rochelle, G. T., Eds.; ACS Symposium Series 188, American Chemical Society: Washington, DC, 1982; pp 153−171.
(17) Lim, P. K.; Huss, A., Jr.; Eckert, C. A. *J. Phys. Chem.* **1982**, *86*, 4233−4237.
(18) Bäckstrom, H. L. J. *Z. Phys. Chem.* **1934**, *B25*, 122−138.
(19) Dogliotti, L.; Hayon, E. *J. Phys. Chem.* **1968**, *72*, 1800−1807.
(20) Lancia, A.; Musmarra, D.; Pepe, F.; Volpicelli, G. *Chim. Ind. (Milan)* **1993**, *75*, 177−181.
(21) Shultz, J. S.; Gaden, E. L. *Ind. Eng. Chem.* **1956**, *48*, 2209−2212.
(22) Sawicki, J. E.; Barron, C. H. *Chem. Eng. J.* **1973**, *5*, 153−159.
(23) Astarita, G. *Mass transfer with Chemical Reaction*; Elsevier: Amsterdam, 1967.
(24) Bates, R. L.; Fondy, P. L.; Corpstein, R. R. *Ind. Eng. Chem. Proc. Des. Dev.* **1963**, *2*, 310−314.
(25) Hughmark, G. A. *Ind. Eng. Chem. Proc. Des. Dev.* **1980**, *19*, 638−641.
(26) Goldberg, R. N.; Parker, V. B. *J. Res. Nat. Bur. Stan.* **1985**, *90*, 341−358.
(27) Brewer, L. In *Flue Gas Desulfurization*; Hudson, J. L., Rochelle, G. T., Eds.; ACS Symposium Series 188; American Chemical Society: Washington, DC, 1982; pp 1−39.
(28) Danckwerts, P. V. *Gas−Liquid reactions*; McGraw-Hill Co.: New York, 1970.
(29) Lancia, A.; Musmarra, D.; Prisciandaro, M.; Tammaro, M. *Chem. Eng. Sci.* **1999**, In press.
(30) Perry, R. H.; Chilton, H. C. *Chemical engineers' handbook*, 5th ed.; McGraw-Hill: Kogakusha, Tokyo, 1973.
(31) Anselmi, G.; Lignola, P. G.; Raitano, C.; Volpicelli, G. *Ozone Sci. Eng.* **1984**, *6*, 17−28.
(32) Abdulsattar, A. H.; Shridar, S.; Bromley, L. A. *AIChE J.* **1977**, *23*, 62−68.
(33) Colin, E.; Clarke, W.; Glew, D. N. *J. Chem. Soc., Faraday Trans.* **1980**, *76*, 1911−1916.

Received for review May 26, 1998. Revised manuscript received February 22, 1999. Accepted February 26, 1999.

ES9805425